Rock and Soil Mechanics

Volume 41 | Issue 7 Article 1

12-22-2020

Study on constitutive model of fractured rock mass based on statistical strength theory

Wei GAO
Key Laboratory of Education for Geomechanics and Embankment Engineering, Hohai University, Nanjing, Jiangsu 210098, China

Cheng-jie HU
Key Laboratory of Education for Geomechanics and Embankment Engineering, Hohai University, Nanjing, Jiangsu 210098, China

Tian-yang HE
Key Laboratory of Education for Geomechanics and Embankment Engineering, Hohai University, Nanjing, Jiangsu 210098, China

Xin CHEN
Key Laboratory of Education for Geomechanics and Embankment Engineering, Hohai University, Nanjing, Jiangsu 210098, China

See next page for additional authors

Custom Citation

GAO Wei, HU Cheng-jie, HE Tian-yang, CHEN Xin, ZHOU Cong, CUI Shuang, . Study on constitutive model of fractured rock mass based on statistical strength theory[J]. Rock and Soil Mechanics, 2020, 41(7): 2179-2188.

Study on constitutive model of fractured rock mass based on statistical strength theory

Authors

Wei GAO, Cheng-jie HU, Tian-yang HE, Xin CHEN, Cong ZHOU, and Shuang CUI

Rock and Soil Mechanics 2020 41(7): 2179−2188 ISSN 1000−7598
https: //doi.org/10.16285/j.rsm.2019.6673 rocksoilmech.researchcommons.org/journal

Study on constitutive model of fractured rock mass based on statistical strength theory

GAO Wei[1, 2], HU Cheng-jie[1, 2], HE Tian-yang[1, 2], CHEN Xin[1, 2], ZHOU Cong[1, 2], CUI Shuang[1, 2]

1. College of Civil and Transportation Engineering, Hohai University, Nanjing, Jiangsu 210098, China

2. Key Laboratory of Education for Geomechanics and Embankment Engineering, Hohai University, Nanjing, Jiangsu 210098, China

Abstract: With the aid of damage mechanics and on the basis of statistical strength theory, a method for establishing the constitutive model of deep fractured rock mass is proposed and verified by laboratory and numerical tests. The fractured rock mass is divided into numerous micro-cubes. The strength of micro-cubes is related to the fracture degree and the strength of each micro-cube is randomly distributed. Thus the strength can be used to reflect the fracture degree of the rock mass. Among them, based on the fact that the work done by friction between fracture surfaces is equal to the strain energy released after the material fracture, the rock fracture degree variable defined from the mechanical point of view is obtained. In addition, it is assumed that the strength distribution of micro-cubes obeys the Weibull distribution and the stress behavior satisfies Hoek-Brown criterion. The constitutive model of fractured argillaceous sandstone rock mass is then established and verified based on typical triaxial test results of fractured rock samples. The results show that the calculated curve from theoretical model is in good agreement with the test results. At last, a supplementary numerical test is carried out using discrete element software PFC, which further proves the good calculation performance of theoretical model for argillaceous sandstone and the feasibility of the constitutive model establishing method proposed in this paper.

Keywords: fractured rock mass; constitutive model; statistical strength theory; Hoek-Brown criterion; Weibull distribution; argillaceous sandstone

1 Introduction

As a natural material with defects, the stress of rock mass is redistributed during the excavation of a deep tunnel, from a three-dimensional stress state to approximately a two-dimensional stress distribution state. Three zones are formed, which are elastic zone, plastic zone and fracture zone, approximately correspond to the elastic stage, plastic stage and post-peak failure stage of the full rock stress-strain curve[1−2]. There are many fracture surfaces and micro-cracks in the surrounding rock of the fracture zone. Many studies have shown that the fractured surrounding rock generally exists in deep-buried tunnels, and the deformation of surrounding rock fracture zone is the main component of total tunnel deformation[3−5]. Therefore, research on the mechanical behavior of surrounding rock in fracture zone is key to ensuring the stability of deep engineering [6].

At present, the research on fractured rock mass in the fracture zone has made some relevant results in terms of laboratory tests, numerical simulations and theoretical models.

In terms of experimental research, Niu et al.[7] conducted a uniaxial compression test on fractured sandy mudstone to study the relationship between the peak strength of rock mass and the development of fracture surface. In addition, Niu [8] also used different post-peak unloading points to prepare rock test samples with different damage degrees in the laboratory, and obtained the strength parameter of each test rock sample through the single specimen method with multiple yields of a single sample and multiple confining pressure levels. Zong[9] studied the reloading mechanical properties of rock samples with different fracture degrees under different stress states and stress paths through reloading tests on rock samples with different fracture degrees, which revealed that the mechanical properties of rock samples vary with the degree of fracture, and that rock transforms from strain softening to strain hardening with increasing fracture degrees. Jin et al. [10] studied the intact rock block and the fractured rock reinforced by grouting cementation and bolt-grouting cementation through laboratory experiments and obtained the mechanical behavior of fractured rock after reinforcement. Because the sample preparation of fractured rock mass has certain difficulties in core drilling and the control of fracture degree, these difficulties have restricted the development of experimental research on fractured rock mass.

In order to obtain mechanical models of fractured rock masses with different fracture degrees, more and more scholars use discrete element numerical methods

Received: 27 September 2019 Revised: 30 December 2019
This work was supported by the National Natural Science Foundation of China (41831278) and the Fundamental Research Funds for the Central Universities (2016B10214).
First author: GAO Wei, male, born in 1971, PhD, Professor, research interests: rock mechanics theories, stability analysis and big data application in engineering. E-mail: wgaowh@163.com

to study the mechanical properties of fractured rock masses. For example, Zhang et al.[11] used the bonded particle model of discrete element software PFC^{2D} for numerical simulation and studied the acoustic emission phenomenon of a single fractured rock sample under different loading modes. Zhu et al.[12] used the 3D Voronoi diagram to establish a three-dimensional broken rock mass model and used the three-dimensional discrete element method program (3DEC) to study the compaction characteristics of the broken rock mass. Bidgoli et al.[13] used the discrete element numerical method (DEM) to carry out a series of numerical tests on the two-dimensional discrete fracture network model to determine the compressive strength of fractured rock mass and study the different properties of fractured rock mass. However, there is currently no calibration method with rigorous theory and convenient operation to obtain the micro parameters corresponding to the macro parameters, which limits the application of the discrete element method in fractured rock masses.

In terms of theoretical models, the exploration of constitutive models of fractured rock masses is still rare, and there are only some preliminary studies. Ge[14] proposed a constitutive model of fractured rock mass based on statistical strength theory. However, the application scope of this model is limited and cannot reflect the mechanical behavior of fractured rock mass in the re-hardening stage due to laboratory test conditions limitation.

Thus, the current research on the fractured rock mass in surrounding rock fracture zone mainly focuses on indoor tests and numerical simulations, but there are few studies on theoretical models. The study on the theoretical model of fractured rock mass should be strengthened as the research is far behind actual engineering application.

Therefore, based on the correlation between rock micro-damage and macro-fracture[15] and drawing inspirations from ideas and methods of damage mechanics, this paper proposes a constitutive model establishment method of fractured rock mass suitable for surrounding rock fracture zone based on statistical strength theory. The corresponding constitutive model was established and verified through typical laboratory test results of argillaceous sandstone fractured rock mass. Finally, the theoretical model is checked by supplementary numerical experiments. This research lays the foundation for in-depth mechanical behavior analysis of surrounding rock in the fracture zone.

2 Establishment of constitutive model for fractured rock mass

2.1 Determination of fracture variable F_t

The process from microscopic damage to macroscopic fracture of rock has good statistical self-similarity[15]. With the aid of damage mechanics method, the fractured rock mass in surrounding rock fracture zone with many randomly distributed fracture surfaces is divided into countless infinitesimal cube of equal size, where the fracture surface is represented by a thick solid line as shown in Fig.1. Under the condition that the number of cubes is unlimited, the percentage of the number of cubes in the broken part to the total number F_t can be expressed by a continuously changing value. The existence of rock fracture surface will inevitably lead to a decrease in strength of the cube. Since the fractured parts are randomly distributed throughout the rock mass, the strength of each cube is also randomly distributed. According to the correlation between the strength of cube and the fracture surface of rock, the stress distribution of the cube can be used to indirectly reflect the fracture degree of the rock mass.

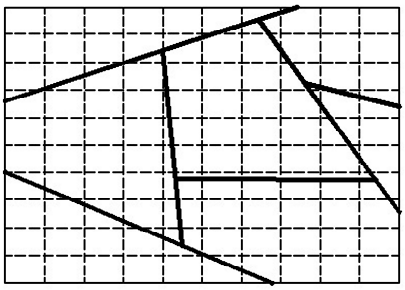

Fig. 1 Conceptual model of fractured rock mass

Assuming that the entire rock mass in the fracture zone is divided into a number of cubes Q and a certain load is applied, the number of broken cubes is Q_c, the fracture degree of the fractured rock mass F_t (referring to the fracture degree of the rock mass after the external load is applied) can be expressed as

$$F_t = \frac{Q_c}{Q} \tag{1}$$

If the strength of the cube obeys a certain probability distribution $P(S)$, the number of damaged cubes whose stress state is within the range $[S, S+\mathrm{d}S]$ after loading is

$$\mathrm{d}Q_c = QP(S)\mathrm{d}S \tag{2}$$

When the stress state is S, the total number of broken cubes is

$$Q_c = \int_0^S Qp(x)\mathrm{d}x = QP(S) \tag{3}$$

Combining Eqs. (1) and (3) can lead to

$$F_t = P(S) \tag{4}$$

The broken rock mass is now abstracted into unbroken part and broken part. The unbroken part is composed of elastic and plastic bodies. The stress of the unbroken part is σ_i' and the stress of the broken part is σ_i'', as

shown in Fig.2. The total stress σ_i of broken rock mass is

$$\sigma_i = \sigma_i'(1-F_t) + \sigma_i'' F_t \ (i=1,3) \tag{5}$$

ε_{ie}' is the strain of elastic body and ε_{ip}' is the strain of plastic body, then the strain of unbroken part of the rock mass ε_i' can be expressed as

$$\varepsilon_i' = \varepsilon_{ie}' + \varepsilon_{ip}' \tag{6}$$

According to the principle of deformation coordination, it is known that

$$\varepsilon_i = \varepsilon_i' = \varepsilon_i'' \tag{7}$$

where ε_i is the total strain of broken rock mass, ε_i' is the strain of unbroken part and ε'' is the strain of broken part.

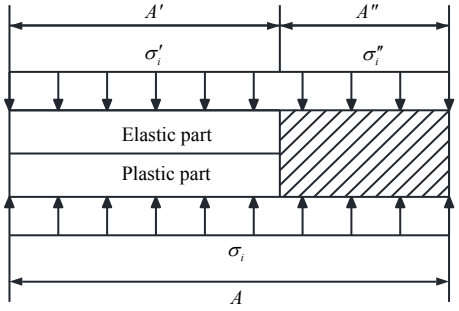

Fig. 2 Mechanical model of fractured rock mass

The elastic part of unbroken rock obeys Hooke's law, and the stress is

$$\sigma_i' = E\varepsilon_{ie}' + \mu(\sigma_j' + \sigma_k') \tag{8}$$

where σ_i', σ_j' and σ_k' are the principal stresses in each direction of the rock mass; E and μ are the elastic modulus and Poisson's ratio of the unbroken part of intact rock sample, respectively.

In the rock mass cyclic loading and unloading test, the unloading modulus does not change much with confining pressure [9]. To simplify the calculation, it is assumed that the unloading modulus E^s at any point on the rock mass stress–strain curve under different confining pressures is a constant value. Then the elastic strain ε_{ie}' of the rock mass satisfies:

$$\varepsilon_{ie}' = \frac{\sigma_i'}{E^s} \tag{9}$$

From Eq. (5), we obtain

$$\left.\begin{aligned}\sigma_1 &= \sigma_1'(1-F_t) + \sigma_1'' F_t \\ \sigma_3 &= \sigma_3'(1-F_t) + \sigma_3'' F_t\end{aligned}\right\} \tag{10}$$

where σ_1 and σ_3 are the maximum and minimum principal stresses of the damaged rock mass, respectively; σ_1' and σ_3' are the maximum and minimum principal stresses of the unbroken part, respectively; σ_1'' and σ_3'' are the maximum and minimum principal stresses of the broken part, respectively.

Assuming the intermediate principal stress of the unbroken part in the triaxial test $\sigma_2' = \sigma_3'$, which is substituted into Eq. (8), we can obtain

$$\sigma_1' = E\varepsilon_{1e}' + 2\mu\sigma_3' \tag{11}$$

Combining Eqs. (9)–(11) can result in

$$\sigma_1 = \frac{2\mu E^s}{E^s - E}\sigma_3 + \left(\sigma_1'' - \frac{2\mu E^s}{E^s - E}\sigma_3''\right)F_t \tag{12}$$

After the failure of rock mass, there is friction and interlocking phenomenon between the fracture surfaces of the rock mass. It is assumed that the rock mass after failure is a friction material and cohesion is not considered, and σ_i'' satisfies Mohr-Coulomb criterion, we have

$$\sigma_1'' = \sigma_3'' \tan^2(\pi/4 + \varphi/2) \tag{13}$$

where φ is the internal friction angle of the fractured rock sample.

For conventional triaxial tests, in the principal stress space, the maximum strain energy that can be released when the rock element fails is [16]

$$\omega_{max} = \frac{(1+\mu)\sigma_c^2}{3E} \tag{14}$$

where ω_{max} is the maximum strain energy and σ_c is the uniaxial compressive strength of intact rock.

The strain energy released by the material after fracture is consumed by friction work done between the rock fracture surfaces [17] (see Fig.3). Considering that the research object in this paper is the fractured rock mass and cohesion is not considered, the energy expression is

$$\omega_c = \frac{N\tan\varphi \cdot \varepsilon_1'}{\sin\alpha} \tag{15}$$

where $N = \sigma_1'' \cos^2\alpha + \sigma_3'' \sin^2\alpha$; ω_c is the frictional energy consumption and α is the angle between the fracture surface and the horizontal plane, assuming $\alpha = \pi/4 + \varphi/2$.

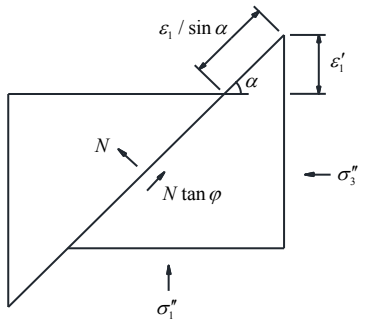

Fig. 3 Mechanical model of rock fracture plane

From Eqs.(7),(13)–(15), and considering $\omega_{max} = \omega_c$, we obtain:

$$\sigma_3'' = k \tag{16}$$

$$\sigma_1'' = k\tan^2\alpha \tag{17}$$

Among them:

$$k=\frac{(1+\mu)\sigma_{\mathrm{c}}^2}{6E\varepsilon_1\tan\varphi\sin\alpha} \tag{18}$$

Substituting Eqs. (16) and (17) into Eq. (12) yields

$$\sigma_1=\frac{2\mu E^{\mathrm{s}}}{E^{\mathrm{s}}-E}\sigma_3+\left(k\tan^2\alpha-\frac{2\mu E^{\mathrm{s}}}{E^{\mathrm{s}}-E}k\right)F_{\mathrm{t}} \tag{19}$$

After transforming Eq. (19), the fracture degree variable is

$$F_{\mathrm{t}}=\frac{(E^{\mathrm{s}}-E)\sigma_1-2\mu E^{\mathrm{s}}\sigma_3}{(E^{\mathrm{s}}-E)k\tan^2\alpha-2\mu E^{\mathrm{s}}k} \tag{20}$$

2.2 Model building

Since Hoek-Brown failure criterion considers the influence of confining pressure on the rock strength, it is more suitable for rock materials. The Hoek-Brown failure criterion is used to express the stress state of the plastic cube of unbroken part in this paper. Considering that the Weibull random distribution function can describe the general law of the meso-uniformity of rock-like materials[18], combined with the Hoek-Brown failure criterion and Weibull distribution, a constitutive model is established based on the statistical strength theory.

The Hoek-Brown criterion expression is

$$\sigma_1=\sigma_3+\sqrt{m\sigma_{\mathrm{c}}\sigma_3+s\sigma_{\mathrm{c}}^2} \tag{21}$$

where m and s are constants related to the rock materials properties.

The Hoek-Brown criterion with constant stress can be expressed as

$$f=m\sigma_{\mathrm{c}}\frac{I_1}{3}+4J_2\cos^2\theta_\sigma+m\sigma_{\mathrm{c}}\sqrt{J_2}\left(\cos\theta_\sigma+\frac{\sin\theta_\sigma}{\sqrt{3}}\right)-s\sigma_{\mathrm{c}}^2 \tag{22}$$

where θ_σ is the Lord's angle, for conventional triaxial tests $\theta_\sigma=30°$; I_1 and J_2 are the first invariant of the stress tensor and the second invariant of the deviator stress, respectively. Under the conditions of the triaxial test $\sigma_2'=\sigma_3'$, there is

$$\left.\begin{aligned}I_1&=\sigma_1'+\sigma_2'+\sigma_3'=\sigma_1'+2\sigma_3'\\J_2&=\frac{1}{3}\left(\sigma_1'-\sigma_3'\right)^2\end{aligned}\right\} \tag{23}$$

From Eqs. (10), (16), (17), we can get

$$\sigma_1'=\frac{2\mu E^{\mathrm{s}}(k\tan^2\alpha\sigma_3-k\sigma_1)}{(E^{\mathrm{s}}-E)(k\tan^2\alpha-\sigma_1)+2\mu E^{\mathrm{s}}(\sigma_3-k)} \tag{24}$$

$$\sigma_3'=\frac{(E^{\mathrm{s}}-E)(k\tan^2\alpha\sigma_3-k\sigma_1)}{(E^{\mathrm{s}}-E)(k\tan^2\alpha-\sigma_1)+2\mu E^{\mathrm{s}}(\sigma_3-k)} \tag{25}$$

Substituting $\theta_\sigma=30°$ into Eq.(22), the average stress level S of the infinitesimal rock cube can be expressed as

$$S=m\sigma_{\mathrm{c}}\frac{I_1}{3}+3J_2+m\sigma_{\mathrm{c}}\sqrt{4J_2/3}-s\sigma_{\mathrm{c}}^2 \tag{26}$$

The probability distribution function of the two-parameter Weibull distribution is

$$P(S)=1-\mathrm{e}^{-(S/F)^t} \tag{27}$$

where t and F are statistical parameters.

Substituting Eqs. (20) and (27) into Eq.(4), that is, the cube strength obeys the Weibull distribution, there is

$$\frac{(E^{\mathrm{s}}-E)\sigma_1-2\mu E^{\mathrm{s}}\sigma_3}{(E^{\mathrm{s}}-E)k\tan^2\alpha-2\mu E^{\mathrm{s}}k}=1-\mathrm{e}^{-(S/F)^t} \tag{28}$$

Substituting Eqs.(18), (26) and $\alpha=\pi/4+\varphi/2$ into Eq (28) leads to

$$\frac{6E\varepsilon_1\tan\varphi\sin(\pi/4+\varphi/2)\left[(E^{\mathrm{s}}-E)\sigma_1-2\mu E^{\mathrm{s}}\sigma_3\right]}{(E^{\mathrm{s}}-E)(1+\mu)\sigma_{\mathrm{c}}^2\tan^2(\pi/4+\varphi/2)-2\mu E^{\mathrm{s}}(1+\mu)\sigma_{\mathrm{c}}^2}=1-\exp\left\{-\left[\left(m\sigma_{\mathrm{c}}\frac{I_1}{3}+3J_2+m\sigma_{\mathrm{c}}\sqrt{4J_2/3}-s\sigma_{\mathrm{c}}^2\right)\Big/F\right]^t\right\} \tag{29}$$

Equation (29) represents the constitutive equation of fractured rock mass based on Hoek-Brown criterion and Weibull distribution under the principal stress, where t and F are newly introduced parameters; m and s are constants related to the rock materials properties in the Hoek-Brown criterion; other parameters such as elastic modulus, unloading modulus, Poisson's ratio and internal friction angle, etc. can be measured through laboratory tests.

2.3 Parameter solving method

2.3.1 Solving method of parameters m and s

The parameters m and s in Hoek-Brown failure criterion are related to the rock type and integrity. For a certain kind of rock, its value is a constant, which can be solved by regression analysis method in mathematical statistics. The calculation process is as follows:

Transforming Eq. (21) can result in

$$(\sigma_1-\sigma_3)^2=m\sigma_{\mathrm{c}}\sigma_3+s\sigma_{\mathrm{c}}^2 \tag{30}$$

For Eq. (30), let

$$\left.\begin{aligned}y&=(\sigma_1-\sigma_3)^2\\x&=\sigma_{\mathrm{c}}\sigma_3\end{aligned}\right\} \tag{31}$$

Then Eq. (30) is transformed into

$$y=mx+s\sigma_{\mathrm{c}}^2 \tag{32}$$

Method for solving m and s is as follows:

By substitute the failure point data of rock triaxial compression test under different confining pressures into Eq.(31), a set of (x, y) can be obtained. After linear fitting, the slope and intercept of the straight line are obtained, and then parameters m and s can be obtained by inversion.

2.3.2 Solving method of parameters t and F

The methods for solving the parameters t and F introduced by Weibull distribution are as follows:

Transform Eq. (28) into

$$1-\frac{(E^{s}-E)\sigma_1-2\mu E^{s}\sigma_3}{(E^{s}-E)k\tan^2\alpha-2\mu E^{s}k}=\mathrm{e}^{-(S/F)^t} \tag{33}$$

Take the logarithm of both sides of Eq. (33) and obtain

$$\ln\left(1-\frac{(E^{s}-E)\sigma_1-2\mu E^{s}\sigma_3}{(E^{s}-E)k\tan^2\alpha-2\mu E^{s}k}\right)=-\left(\frac{S}{F}\right)^t \tag{34}$$

Then taking the logarithm of both sides of equation (34), we obtain

$$\ln\left[-\ln\left(1-\frac{(E^{s}-E)\sigma_1-2\mu E^{s}\sigma_3}{(E^{s}-E)k\tan^2\alpha-2\mu E^{s}k}\right)\right]=t\ln S-t\ln F \tag{35}$$

For Eq. (35), let

$$\left.\begin{aligned} y&=\ln\left[-\ln\left(1-\frac{(E^{s}-E)\sigma_1-2\mu E^{s}\sigma_3}{(E^{s}-E)k\tan^2\alpha-2\mu E^{s}k}\right)\right]\\ x&=\ln S\\ a&=t\\ b&=-t\ln F \end{aligned}\right\} \tag{36}$$

where a is the slope and b is the intercept.

Then the Eq. (35) is equivalently transformed into a linear equation, as

$$y=ax+b \tag{37}$$

Substitute the data from the full stress–strain test of the broken rock mass into the first two expressions of Eq. (36) to obtain a set of data (x, y), and calculate the slope a and intercept b of the straight line after linear fitting of the data, and then obtain the parameters t and F according to the last two formulas of Eq. (36).

3 Experimental verification of fractured rock mass constitutive model

For different types of rock masses, the parameters m and s of Hoek-Brown failure criterion and the parameters t and F introduced by the Weibull distribution in Eq.(29) are different. The corresponding parameter values need to be determined through laboratory triaxial compression tests to obtain the constitutive equation of the corresponding rock mass.

Zong's [9] reloading test on argillaceous sandstone samples at the residual failure stage is in good agreement with the research objective of this article. Therefore, the constitutive equation of fractured argillaceous sandstone rock mass is established here to verify its applicability, and further, prove the feasibility of the establishing method of constitutive model. The full stress-strain curve obtained by Zong's experiment [9] is shown in Fig.4.

3.1 Model establishment

3.1.1 Solving parameters m and s

The failure data points of fractured argillaceous sandstone samples under different confining pressures are obtained from Fig. 4, and (x, y) is calculated by Eq. (31). The results are shown in Table 1. The linearly fitted results of data (x, y) are plotted in Fig. 5.

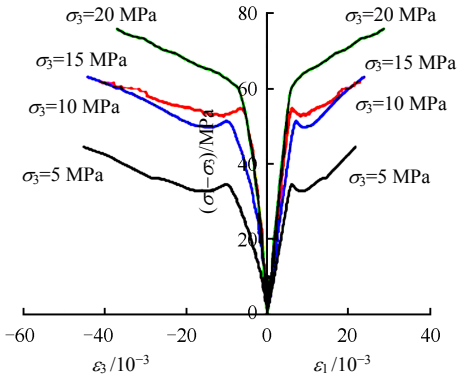

Fig. 4 Complete stress-strain curve of reloaded rock specimen [9]

Table 1 Failure data of fractured rock under different confining pressures

σ_1 /MPa	σ_3 /MPa	x	y
39.82	5	346.10	1 218.68
61.53	10	692.20	255.28
70.06	15	1 038.30	3 031.47
80.94	20	1 348.40	3 713.83

By fitting, we obtain $m=2.28$, $s\sigma_c^2=683.40$. When $\sigma_c=69.22$ MPa, we have $m=2.28$、$s=0.14$.

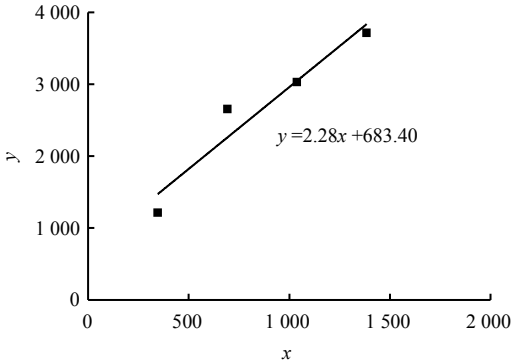

Fig. 5 Linear fitting results

3.1.2 Solving parameters t and F

The stress-strain test data points of the fractured argillaceous sandstone sample in Fig.4 at different confining pressures are sorted and calculated according to the first two formulas of Eq.(36), and obtaining $(x_i,\ y_i)\ i=1,2,3,\cdots n$,where n is the test data sample size. Linear fitting is performed on the sorted data to obtain the slope and intercept of fitted line, namely a and b, and then derive the parameters t and F according

to the last two expressions of Eq. (36). The calculation results are listed in Table 2.

Table 2 Statistical parameter fitting results of reloading test

Failure criterion	Confining pressure / MPa	t	F/ MPa
H-B Criterion	5	1.743	515.934
	10	2.291	534.834
	15	2.361	608.740
	20	2.522	628.276

Taking σ_3 as the function independent variables, and the parameters t and F in Table.2 as the dependent variables, the data scatter plots describing the σ_3-t relationship and the σ_3-F relationship are shown in Fig.6. The modified equations of parameters t, F and σ_3 are obtained by mathematical fitting regression analysis method, namely

$$\left.\begin{aligned} t &= 1.244\ 1\times\ln\left(2.571\ 8\times\ln\sigma_3\right) \\ F &= 460.363\ 3+9.280\ 6\sigma_3 \end{aligned}\right\} \tag{38}$$

According to the fitting results corresponding to the fractured argillaceous sandstone rock mass, the Weibull distribution parameter t has a logarithmic function relationship with σ_3, and the parameter F has a linear relationship with σ_3. The correlation coefficients are 0.957 47 and 0.900 75, respectively, displaying a relatively good fitting. Substituting Eq. (38) into Eq.(29), a constitutive equation of fractured argillaceous sandstone rock mass based on the Hoek-Brown failure criterion and Weibull distribution under the expression of principal stress can be obtained as

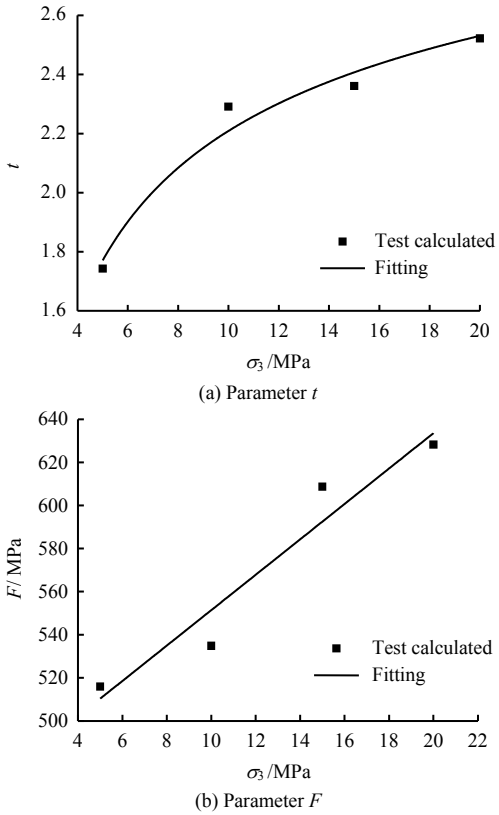

Fig. 6 Relationship between Weibull distribution parameters and confining pressure σ_3

$$\frac{6E\varepsilon_1\tan\varphi\sin(\pi/4+\varphi/2)\left[(E^{\mathrm{s}}-E)\sigma_1-2\mu E^{\mathrm{s}}\sigma_3\right]}{(E^{\mathrm{s}}-E)(1+\mu)\sigma_{\mathrm{c}}^2\tan^2(\pi/4+\varphi/2)-2\mu E^{\mathrm{s}}(1+\mu)\sigma_{\mathrm{c}}^2}= 1-\exp\left\{-\left[\left(m\sigma_{\mathrm{c}}\frac{I_1}{3}+3J_2+m\sigma_{\mathrm{c}}\sqrt{4J_2/3}-s\sigma_{\mathrm{c}}^2\right)\Big/\left(460.363\ 3+9.280\ 6\sigma_3\right)\right]^{1.244\ 1\times\ln(2.571\ 8\times\ln\sigma_3)}\right\} \tag{39}$$

The sample studied in this paper is argillaceous sandstone. According to Zong's s test data, the values of the parameters in Eq.(39) are as following: E^{s} = 15.96 GPa, E=11.84 GPa, μ=0.43, φ=30.51°, c= 31.31 MPa, $\sigma_{\mathrm{c}}=69.22$ MPa, $m=2.28$ and $s=0.14$.

3.2 Model verification

The calculation results of theoretical model are compared with the indoor test results, as shown in Fig.7. Since the default material is a linear elastic material in the initial stage and the stress-strain curve is linear, the model has a large error in the initial stage.

Figure 7 shows that the constitutive equation of fractured argillaceous sandstone rock mass developed in this paper can better reflect the actual mechanical behavior of rock in the fracture zone of argillaceous sandstone. The initial deformation modulus and peak strength are roughly the same as the ones of the test, and the model curve are basically consistent with test results. When the confining pressure is low, the theoretical strain value of the model has a large gap with the actual strain value of the same stress value, but as the confining pressure increases, the gap between the two becomes smaller. The model curve simulates the test results more accurately with the increase of confining pressure.

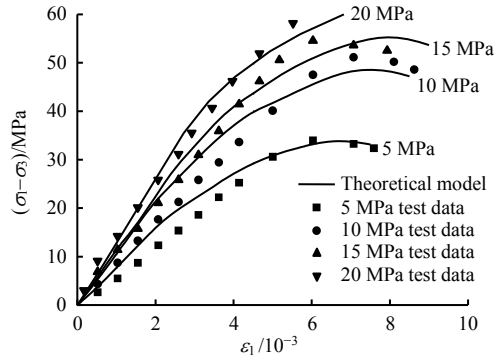

Fig. 7 Comparison between theoretical curves and test data

In order to perform an in-depth analysis of the calculation quality of the model, the model deviation

is analyzed here, and the calculation formula is as follows:

$$\delta = \frac{\sum_{i=1}^{n'} \left| \sigma_i^{\mathrm{T}} - \sigma_i^{\mathrm{E}} \right|}{n'} \tag{40}$$

$$\bar{\delta} = \frac{\sum_{i=1}^{n'} \left| \sigma_i^{\mathrm{T}} - \sigma_i^{\mathrm{E}} \right|}{\sum_{i=1}^{n'} \sigma_i^{\mathrm{E}}} \times 100\% \tag{41}$$

where δ and $\bar{\delta}$ are the absolute deviation and the relative deviation, respectively; σ_i^{E} are the experiment value; σ_i^{T} are the theoretical model values that corresponding strain of the same σ_i^{E}; and n' are the number of data points. The calculation results are shown in Table 4.

Table 4 Deviation results of model

Failure Criterion	Confining pressure /MPa	Absolute deviation δ/MPa	Relative deviation $\bar{\delta}$ /%
H-B Criterion Weibull Distribution	5	2.59	14.79
	10	3.19	11.15
	15	1.81	5.26
	20	1.33	3.56

It can be seen from Table 4, at low confining pressure, although the absolute deviation between the theoretical value of the model and the experimental value slightly increases, the absolute deviation generally decreases, and the relative deviation of the model decreases with increasing confining pressure. When the confining pressure is 20 MPa, the relative deviation is below 5%, and the theoretical curve of the model is in good agreement with the test results. The model deviation decreases with the increase of confining pressure. The reason is that the constitutive model parameters proposed in this paper use the elastic modulus of intact rock, while the actual experiment is the elastic modulus of fractured rock mass. There is a certain gap between the two. And, the modulus of elasticity during the test increases with the increase of confining pressure, and the gap between the theoretical modulus and the experimental modulus becomes smaller. Therefore, the deviation of the model data also decreases.

4 Numerical verification of the fractured rock mass constitutive model

Since the laboratory test is only the result of fractured rock sample with a single penetrated fracture surface, the degree of rock mass fracture is low. Therefore, this paper aims to establish numerical models of fractured argillaceous sandstone samples with different fracture states using the discrete element software PFC, to comprehensively verify the applicability of fractured argillaceous sandstone constitutive model and the feasibility of method for establishing the constitutive model with aid of numerical tests.

4.1 Establishment of numerical model

Using the results of Zong's laboratory experiment[9], the microscopic parameters of argillaceous sandstone numerical model were calibrated. The experimental processing method of numerical study is the same as that in Zong's literature. First, establish an intact rock sample model, load it until break and unload to obtain a fractured rock sample, and then perform a reload test on fractured rock sample under different confining pressures. The model adopts a parallel bonding model. By constantly adjusting the micro-parameters, the stress-strain curves similar to the test results were achieved. Figure 8 shows the comparison of curves between numerical test and laboratory test. Figure 9 illustrates the comparison between the fractured rock sample model and the laboratory test rock sample before reloading. The fractured rock samples were subjected to reloading tests under different confining pressures, and the comparison between numerical and laboratory test stress–strain curve is plotted in Fig.10. The calibration results of microscopic parameters are shown in Table 5.

From Fig.8 and Fig. 10, it can be found that the numerical test results of uniaxial compression and triaxial compression are basically consistent with the laboratory test results, and the macroscopic phenomena shown by the corresponding microscopic parameters are basically consistent with laboratory test results. It shows that the calibration results of argillaceous sandstone microscopic parameters are good, and the parameters in Table 5 are reasonable and valid.

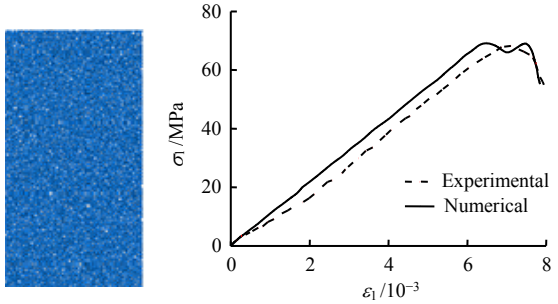

(a) Numerical model (b) Stress-strain curves

Fig. 8 Uniaxial compression test of intact argillaceous sandstone specimen

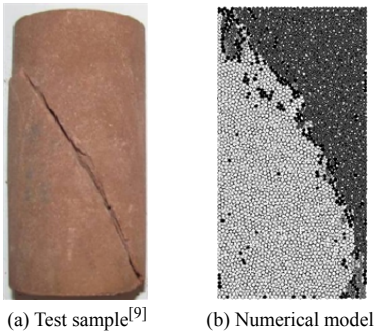

(a) Test sample[9] (b) Numerical model

Fig. 9 Comparative diagrams of laboratory specimen and numerical model of fractured rock mass for argillaceous sandstone

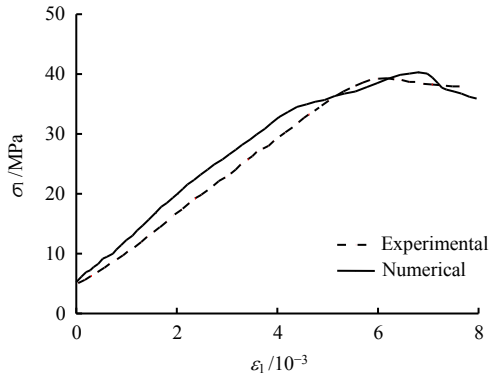

(a) σ_3=5 MPa

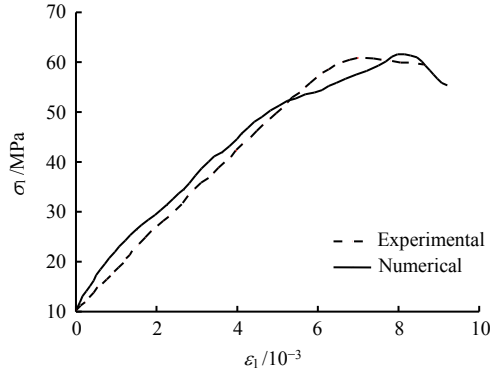

(b) σ_3=10 MPa

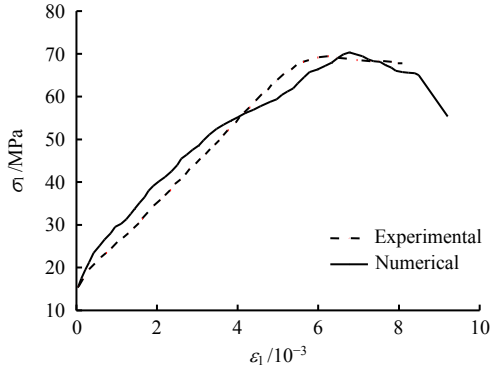

(c) σ_3=15 MPa

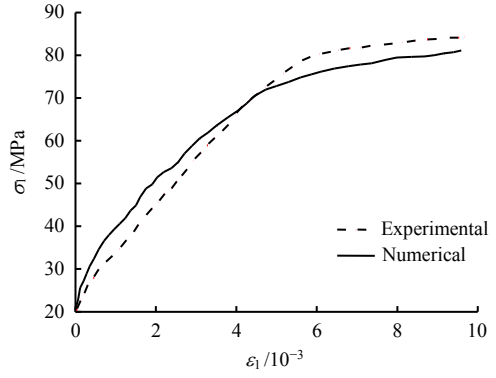

(d) σ_3=20 MPa

Fig. 10 Comparative diagrams between numerical simulation and laboratory test

Table 5 PFC microparameters

Effective modulus E^*/GPa	Stiffness ratio k^*	Radius multiplier λ	Radius ratio R_{max} /R_{min}	Friction coefficient μ^*	Porosity	Bond strength /MPa
5	1	1	1.5	0.577	0.1	25

Although the deformation modulus of numerical curve is slightly deviated, the trend of curve is basically the same as the test curve, and the peak strength is roughly the same. At the same time, as the confining pressure increases, the model also changes from strain softening to strain hardening. There is a certain deviation between the deformation modulus of numerical and experimental curve. This is because the model only approximates some large and obvious cracks, while ignoring many microscopic cracks in the real rock sample, which leads to a fact that the deformation modulus of the simulated fractured rock samples is higher than the one from the laboratory test under the same confining pressure in the initial stage before peak.

4.2 Numerical verification of rock samples with large fracture degree

Triaxial loading test (σ_3=50 MPa) is performed on intact argillaceous sandstone sample. When loading reaches the residual stage, it is unloaded to obtain a rock sample with a greater degree of fracture. The rock sample is subjected to different confining pressures (5, 10, 15, 20, 25, 30 MPa) in reload test. The numerical and test results are shown in Fig.11. The model in Fig. 11(a) has obvious fracture surfaces and fissures, and the rock fracture degree is relatively high. Compared with the test results of intact rock sample in Fig.10, the test results of the highly fractured rock sample in Fig.11(b) show that the peak strength of highly fractured rock sample is significantly lower under the same confining pressure.

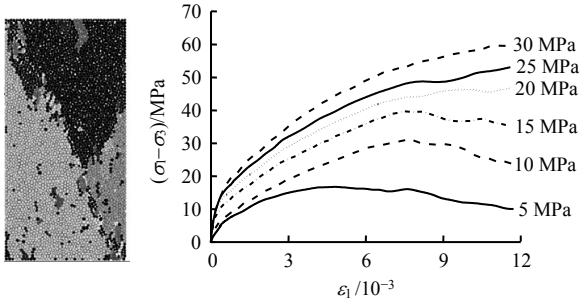

(a) Numerical model (b) Stress-strain curves

Fig. 11 Simulation results of rock specimen with multiple fracture planes

The theoretical model is verified based on the numerical test results. In the case of triaxial test, the comparison between theoretical curve and numerical test curve of fractured argillaceous sandstone sample is shown in Fig. 12.

Figure 12 presents that the theoretical curve of the fractured argillaceous sandstone sample is roughly consistent with the overall trend of the test curve, which can exhibit the elastic stage, plastic stage and strain softening stage of the rock well. However, the theoretical model curve has a certain deviation from the experimental data at the initial stage. This is

because the model assumes that the rock is a linear elastic body at the initial stage, while actual test sample is a fractured rock with many cracks, and the initial compaction stage is inelastic. This is quite different from the initial stage of the numerical model curve.

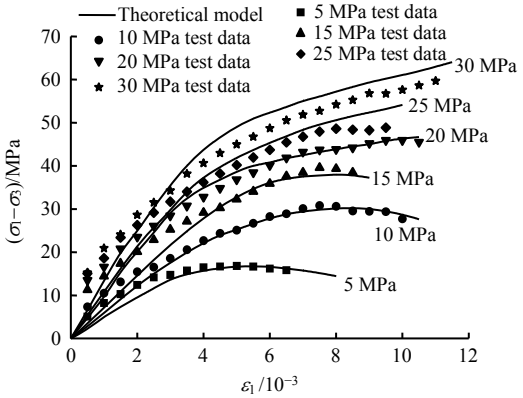

Fig. 12 Comparison between theoretical curve and test data of rock specimen model with multiple fracture planes

4.3 Numerical verification of rock samples with small fracture degree

The applicability of the model to rock samples with lower fracture degrees is verified. The intact argillaceous sandstone sample is loaded to 80% stress post peak under a confining pressure of 30 MPa and unloaded to obtain a fractured rock sample with non-penetrating fracture surface. The rock samples were reloaded under different confining pressures (5, 10, 15, 20, 25, 30 MPa). The numerical and test results are shown in Fig. 13. Compared with the rock model with large fracture degree in Fig. 11(a), the rock model with small fracture degree in Fig. 13(a) has fewer cracks, only one larger fracture surface, and smaller fracture degree. Compared with the test results of the large fractured rock sample in Fig.11(b), the peak strength of lower fractured rock is higher under the same confining pressure, and the peak strength of lower fractured rock sample is higher at high confining pressure. The rock sample with lower fracture degree also appears to be strain hardening under higher confining pressure.

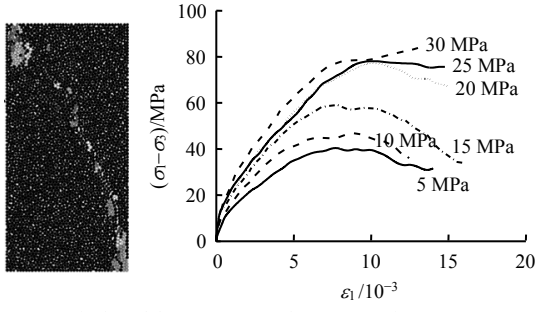

(a) Numerical model (b) Stress-strain curve

Fig. 13 Simulation results of rock specimen with small fracture degree

The theoretical model is verified based on the numerical test results. The comparison between theoretical curve and numerical test curve of fractured argillaceous sandstone sample is shown in Fig. 14.

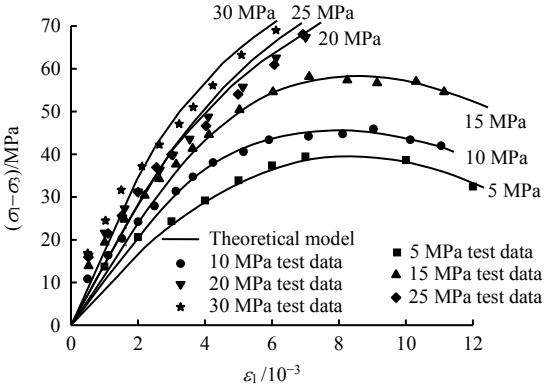

Fig. 14 Comparison between theoretical curves and test data of rock specimen model with small fracture degree

It can be found from Fig.14 that the theoretical model curve is in good agreement with the experimental data, the peak strength values are basically the same, and the curve trends are also the same, which can well reflect the various stages of rock failure.

Comparing Fig. 12 and Fig.14, it can be found that the theoretical model curve of the rock sample with small fracture degree is in better agreement with experimental data. This is because the constitutive model uses the elastic modulus of intact rock, which is greater than the elasticity of fractured rock mass in the actual test. The elastic modulus of the rock sample with small fracture degree is greater than that of large fracture degree and is closer to the elastic modulus of intact rock. In the figure, the curve of small fracture degree model is more consistent with the experimental data.

Numerical test verification of the above two fractured argillaceous sandstone samples with different fracture degrees can prove that the constitutive model of fractured argillaceous sandstone established in this paper can well reflect the mechanical behavior of rock samples with different fracture degrees. This model has high applicability, further proving the feasibility of method for establishing the theoretical model of fractured rock mass.

5 Conclusion

The fracture degree variable of fractured rock mass is defined from mechanical point of view. The theoretical fracture degree of rock mass can be calculated from triaxial test data, which reflects the relationship between the degree of rock fracture and the strength of rock itself;

Establishing the corresponding fractured rock mass constitutive model based on the triaxial test data of fractured argillaceous sandstone. The calculated

results are in good agreement with the test curve, and the relative deviation between the two decreases as the confining pressure increases. The relative deviation is less than 5% under a high confining pressure. PFC numerical test is used to verify the fractured rock of two argillaceous sandstone with different fracture degrees, which proves the applicability of the model.

As the confining pressure increases, the stress−strain curve of fractured argillaceous sandstone changes from strain softening to strain hardening; and Weibull distribution parameters *t* and *F* increase with the increase of σ_3.

(4) Through the verification of the constitutive model of argillaceous sandstone fractured rock mass, the feasibility of the method for establishing the constitutive model of fractured rock mass in this paper is proved.

The experimental sample used in this paper is only argillaceous sandstone, and it is only tested in conventional triaxial tests. Therefore, the obtained constitutive model is only suitable for describing the behavior of argillaceous sandstone fractured rock mass under different confining pressures of conventional triaxial test. For other rock types and test conditions, fitting can be performed according to the same method to obtain the corresponding constitutive model. In addition, the test sample in this article is a fractured rock mass with many randomly distributed fracture surfaces and micro-cracks. If the fracture surfaces or microfractures are not entirely randomly distributed, the method in this paper needs to be improved.

Reference

[1] JING Hong-wen, LI Yuan-hai, XU Guo-an, et al. Analysis of displacement of broken surrounding rock of deep roadway[J]. Journal of China University of Mining & Technology, 2006, 35(5): 565−570.

[2] DONG Fang-ting, SONG Hong-wei, JIN Hong-wen, et al. Supporting theory and application technology of rock mass around tunnel[M]. Beijing: China Coal Industry Publishing House, 2001.

[3] CHEN M, LU W B, YAN P, et al. Blasting excavation induced damage of surrounding rock masses in deep-buried tunnels[J]. KSCE Journal of Civil Engineering, 2016, 20(2): 933−942.

[4] ZHU Z M, WANG C, KANG J M, et al. Study on the mechanism of zonal disintegration around an excavation[J]. International Journal of Rock Mechanics & Mining Sciences, 2014, 67: 88−95.

[5] GAO Qiang, ZHANG Qiang-yong, ZHANG Xu-tao, et al. Zonal disintegration mechanism analysis based on strain gradient of deep surrounding rock mass under dynamic unloading effect[J]. Rock and Soil Mechanics, 2018, 39(9): 3181−3194.

[6] ZHANG Zhen-quan. The study on temporal and spatial evolution characteristics of surrounding rock stress shell of deep roadway and supporting mechanism[D]. Beijing: China University of Mining and Technology (Beijing), 2018.

[7] NIU Shuang-jian, JING Hong-wen, YANG Da-fang, et al. Experimental study on strength characteristics and deformation behavior of the cracked rock samples under uniaxial compression[J]. Journal of Mining & Safety Engineering, 2015, 32(1): 112−118.

[8] NIU Shuang-jian, JING Hong-wen, YANG Xu-xu, et al. Experimental study of strength degradation law of surrounding rock in fractured zone of deep roadway[J]. Chinese Journal of Rock Mechanics and Engineering, 2012, 31(8): 1587−1596.

[9] ZONG Yi-jiang. Study on creep mechanical properties and constitutive model of deep cracked surrounding rock[D]. Xuzhou: China University of Mining and Technology, 2013.

[10] JIN Ai-bing, WANG Zhi-kai, MING Shi-xiang. Experimental investigation on mechanical property of reinforced fractured rock[J]. Chinese Journal of Rock Mechanics and Engineering, 2012, 31(Suppl. 1): 3395−3398.

[11] ZHANG X P, ZHANG Q, WU S C. Acoustic emission characteristics of the rock-like material containing a single flaw under different compressive loading rates[J]. Computers & Geotechnics, 2017, 83: 83−97.

[12] ZHU De-fu, TU Shi-hao, YUAN Yong, et al. An approach to determine the compaction characteristics of fractured rock by 3D discrete element method[J]. Rock and Soil Mechanics, 2018, 39(3): 1047−1055.

[13] BIDGOLI M N, ZHAO Z H, JING L R. Numerical evaluation of strength and deformability of fractured rocks[J]. Journal of Rock Mechanics and Geotechnical Engineering, 2013, 5(6): 419−430.

[14] GE Ming-ming. Preliminary study on mechanical behavior and constitutive model of fractured rock mass[D]. Nanjing: Hohai University, 2015.

[15] GAO Feng, XIE He-ping, WU Jing-bo. Fractal analysis of the relation between rock damage and rock fragmentation[J]. Chinese Journal of Rock Mechanics and Engineering, 1999, 18(5): 497−502.

[16] WANG Xiang-dong, DENG Ai-min. Mechanics of materials[M]. Beijing: China Water & Power Press, 2014.

[17] CAO Wen-gui, ZHANG Sheng, ZHAO Ming-hua, et al. Study on statistical damage constitutive model of rock based on new definition of damage[J]. Rock and Soil Mechanics, 2006, 27(1): 41−46.

[18] YANG Yue-feng. Simulation based research on crack propagation mechanism of rock like materials under dynamic stress[D]. Dalian: Dalian University of Technolology, 2013.